Precise Radial Un-distortion of Images

John Mallon, Paul F. Whelan
Vision Systems Group, Dublin City University, Ireland
john.mallon@eeng.dcu.ie

Abstract

Radial image distortion is a frequently observed defect when using wide angle, low focal length lenses. In this paper a new method for its calibration and removal is presented. An inverse distortion model is derived that is accurate to a sub-pixel level, over a broad range of distortion levels. An iterative technique for estimating the models parameters from a single view is also detailed. Results on simulated and real images clearly indicate significantly improved performance compared to existing methods.

1. Introduction

Geometric image distortion is an inevitable result of compound lenses. Lens manufacturers consider its compensation subject to many other chromatic and monochromatic aberrations. As a consequence, especially in wide angle lenses, distortion is in evidence on the image surface. Its presence results in a geometric shift of an image point from that of the predicted gaussian optics. Its well known nature is radial dependent about a principle point, producing barrel or pin-cushion effects.

In contrast with the lens manufacturer, we are in a situation where the complete removal of distortion is feasible by pre-calibrating the image array. Distortion removal has numerous implications for single and multi-camera systems, not least in their calibration. This is a consequence of validating the underlying perspective projection assumption.

Understandably, a large amount of effort has been directed at the problem. Initially the photogrammetric community developed methods for modelling and removing distortion [11, 8, 1]. Notable here is the plum line technique of Brown [4] where distortion is calibrated using a setup of straight wires. The baton has been taken up by computer vision, where the same ideas are implemented using straight edge segments [6, 14]. In the calibration realm its removal is considered in conjunction with orientation and lens or internal estimation [18, 15, 17].

The above mentioned implementations use what we believe to be an approximation to the true mathematical model of distortion. Considering alternate interpretations and models [16], un-doubtably an air of confusion surrounds distortion, illustrated for example by [13]. However, when derived from the optics wave abberation equation [2], distortion is modelled as the mapping from ideal gaussian to image plane co-ordinates, via a radial dependent odd order polynomial. This rises the issue of finding an inverse function for distortion. However, it is not analytically invertible and an approximation must be used. Finding such an approximation is the main aim of this paper.

Inverse approximations have been proposed, most notable by Heikkila [9] where an approximation of a taylor expansion including first order derivatives is given. Wei and Ma [17] and Heikkila and Silven [10] both investigated using implicit rational polynomials to approximate the inverse, but are in general unstable and hence not appropriate.

In this paper we derive an inverse function for radial distortion based on a first order taylor expansion, followed by a reformulation which allows the function converge to approximate the inverse to a typical Euclidean error band of ± 0.5 pixels over a wide range of distortion levels.

In section 2, we briefly outline the notation used and present the model of distortion. An inverse to this model is derived in section 3, with experimental results in section 4.

2. Distortion model

The ideal projection of a three dimensional object point is represented on the image plane as an undistorted point, $p_u = (x_u, y_u)^T$. Its corresponding distorted point is $p_d = (x_d, y_d)^T$. Radial distances are similarly represented by $r_u = \sqrt{x_u^2 + y_u^2}$ and $r_d = \sqrt{x_d^2 + y_d^2}$ for ideal and distorted points. Multivariate functions are represented in concise form, for example $f_u = (f_x(x_u, y_u), f_y(x_u, y_u))^T$.

There are two types of distortion affecting an image: radial and tangential. Tangential distortion stems from misalignments of the lens optics, resulting in a geometric shift

Proceedings of the 17th International Conference on Pattern Recognition (ICPR'04)
1051-4651/04 $ 20.00 IEEE

of the image along, and tangential to, the radial direction through the principle point. Its mathematical model was derived by Conrady [5] as used by Brown [3], but has received scant attention in optics texts. It is not readily observed on images, especially in the presence of radial distortion. We do not consider it in this paper for two reasons: it is unclear as to it presence, and small levels can be somewhat reduced by a variable principle point [12]. Secondly, it simplifies the inverse distortion model in terms of complexity. Note however, that it is also invertible in the manner presented in this paper.

Radial distortion is the result of a tradeoff in the lens between many abberations including spherical abberation, coma, astigmatism and field curvature. It is present to a visible level in wide angle or low focal length lenses. Its mathematical model can be derived from the wave abberation function [2, 7], though for reasons of space we do not present this here. Distorted points are related to undistorted points by the infinite series:

$$p_d = p_u + k_1 r_u^3 + k_2 r_u^5 + k_3 r_u^7 + ...,$$

where k_n are scaler coefficients. In our experience we have found that in the noise affected image space, there is no improvement in the modelling of distortion with more than the fifth order relation:

$$p_d = p_u + f_u, \tag{1}$$

where

$$\begin{aligned} f_x(x_u, y_u) &= k_1 x_u r_u^2 + k_2 x_u r_u^4, \\ f_y(x_u, y_u) &= k_1 y_u r_u^2 + k_2 y_u r_u^4. \end{aligned}$$

In general k_1 is dominant over k_2. If $k_1 < 0$ barrel distortion is observed with $k_1 > 0$ for pincushion distortion.

3. Inverse distortion model

Given distorted image coordinates, eq.(1) offers no route to undistort the image array. Clearly an inverse function is required. The model described by eq.(1) is not analytically invertible, nor does it offer any obvious clues as to the likely form the inverse might take. An approximation is required.

The most common approach to inverting the forward model is equivalent to taking the first term in the taylor expansion of eq.(1) and re-estimate the parameters [6, 1, 18, 17, 14] as follows:

$$p_u = p_d - f_d. \tag{2}$$

This is sometimes assumed to be the actual model and indeed suffices for small distortion levels. Heikkila and Silven [10] and indirectly Wei and Ma [17] have used implicit bivariate rational polynomials to approximate the inverse function given data vectors of distorted and undistorted points. Heikkila and Silven further refine the resulting polynomial to reduce the parameter space giving better performance. We have found these techniques to become unstable easily with a change in distortion level and in theory are not suitable due to the lack of Weierstrass's Polynomial Theorem for such multivariate problems. Heikkila [9] proposed an inverse approximation based on the inclusion of a quantity of the first and second terms of the taylor expansion. Our results are compared to this model and that of eq.(2).

Our inverse is based on the first and second terms of the taylor expansion of the forward model i.e. eq.(1). Assuming that the inverse function for f_u is g_d, they can be related by the taylor expansion of f_u about points p_d as:

$$g_d = f_d + \frac{\partial f_d}{\partial x}(x_u - x_d) + \frac{\partial f_d}{\partial y}(y_u - y_d) + H.O.T.$$

Neglecting the higher order terms (due to complexity) the approximate becomes:

$$\begin{aligned} x_u &= x_d + \left(\frac{-f_x + f_y \frac{\partial f_x}{\partial y} - f_x \frac{\partial f_y}{\partial y}}{1 + \frac{\partial f_x}{\partial x} + \frac{\partial f_y}{\partial y}} \right), \\ y_u &= y_d + \left(\frac{-f_y + f_x \frac{\partial f_y}{\partial x} - f_y \frac{\partial f_x}{\partial x}}{1 + \frac{\partial f_x}{\partial x} + \frac{\partial f_y}{\partial y}} \right). \end{aligned} \tag{3}$$

For small values of distortion the following assumption can be made:

$$p_u = p_d - \left(\frac{f_d}{1 + \frac{\partial f_x}{\partial x} + \frac{\partial f_y}{\partial y}} \right), \tag{4}$$

which is equivalent to that proposed by Heikkila [9]. This assumption is useful as it biases the approximation closer to the actual inverse than that of eq.(3) after re-estimation of the parameters. Evaluation of eq.(3) results in:

$$p_u = p_d - p_d \left(\frac{k_1 r_d^2 + k_2 r_d^4 + k_1^2 r_d^4 + k_2^2 r_d^8 + 2 k_1 k_2 r_d^6}{1 + 4 k_1 r_d^2 + 6 k_2 r_d^4} \right).$$

We now refine this model in order that it may approximate the inverse g_d better than eq.(3). In this respect the parameters of the denominator are allowed independence from k_1 and k_2 in an effort to model the denominator of the higher ordered expansion. This significantly improves the models approximation of the inverse. Additionally, the numerator is adjusted to be linear in parameters. (The latter modification has a smaller impact in relation to the former and may be omitted to reduce the parameter space). The resulting formulation of the inverse approximation now becomes:

$$\begin{aligned} p_u &= p_d + \delta_d, \\ \delta_d = \frac{\beta}{\alpha} &= \frac{-p_d \left(a_1 r_d^2 + a_2 r_d^4 + a_3 r_d^6 + a_4 r_d^8 \right)}{1 + 4 a_5 r_d^2 + 6 a_6 r_d^4}. \end{aligned} \tag{5}$$

The performance of three inverse formulations described by eq.(2), eq.(4) and eq.(5) on simulated noise free data is shown in figure 1. The data is planar, normalised to $-0.5 \rightarrow 0.5$ and distorted according to eq.(1). Distortion is stepped through a range of $k_1 = -0.5 \rightarrow 0.5$ and $k_2 = k_1/2$, where the outer values represent severe distortion as present on fish eye lenses.

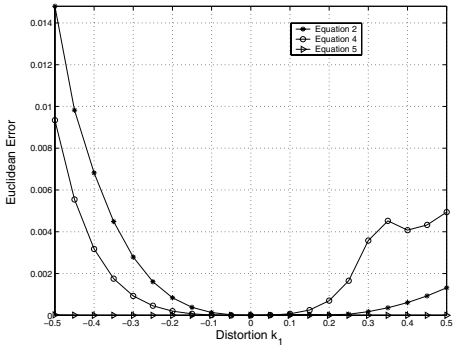

Figure 1. Normalised mean perimeter Euclidean error on noise free data, for a range of distortion levels.

3.1. Parameter estimation

Estimating the parameters of the inverse model described in eq.(5) could be done linearly, only the undistorted data is unobservable in an image. Because of this an iterative estimation approach is taken to minimise an error quantity. This quantity is based on a truism, for example, straight lines project to straight lines [6, 4, 14]. In our experiments we use planar surfaces whose projection in a image must also be planar.

The image surface coordinates are converted to frame buffer coordinates by:

$$x_d = \frac{x_{\tilde{n}} + x_o}{s}, \qquad y_d = y_{\tilde{n}} + y_o,$$

where $x_{\tilde{n}}$ and $y_{\tilde{n}}$ are the frame coordinates, usually normalised by the image width or height. The principle point is denoted by (x_o, y_o) and s accounts for the aspect ratio. A Gauss-Newton iterative estimation procedure is outlined as:

$$\begin{aligned} e^k &= p^k_{\tilde{u}} - h_{ls}(p^k_{\tilde{u}}), \\ \phi^{k+1} &= \phi^k - \lambda H^k \nabla^k e^k, \\ p^{k+1}_{\tilde{u}} &= p^k_d + \delta_d(\phi^{k+1}), \end{aligned} \tag{6}$$

where $p_{\tilde{u}}$ are the estimated undistorted points, h_{ls} is a least squares plane to plane projective transformation or homography. $\phi = [a_1, ..., a_6, x_o, y_o, s]^T$ is the parameter vector and $H = [\nabla^T \nabla]^{-1}$ is the Hessian, with the gradient approximated as $\nabla \cong \frac{\partial p_{\tilde{u}}}{\partial \phi}$. $\delta_d(\phi^{k+1})$ is the evaluation of eq(5) with the current parameter estimate ϕ^{k+1}.

4. Experimental results

The aim of these experiments is to evaluate the performance of the proposed inverse function on real data. The experiments are carried out on noise corrupted simulated data and real images. Errors are based only on points at the perimeter of the images since it is easier to undistort central points and we wish to avoid their biasing influence. Quantifiable results are available in two forms for simulated data: perimeter Euclidean error based on the original undistorted points and a perimeter Euclidean error based on the objective function e^k in eq.(6). For real images only the objective function error is available.

The accuracy of the inverse function in real situations is limited by the noise level in the feature detection and in turn the image. The noise variance found through repeated sampling is used as noise variance in simulated data to evaluate the stability and performance of the proposed inverse function in comparison to those of eq.(2) and eq.(4). Consequently, Figure 2 demonstrates the behaviour in response the expected noise level (± 0.5 pixels), for both error quantities, with data normalised to 1. Only barrel distortion is considered as it is the commonest form. The proposed model shows a significantly reduced error and is the only model to exhibit error within the ± 0.5 pixel bound, in approximating undistorted points over the entire distortion range.

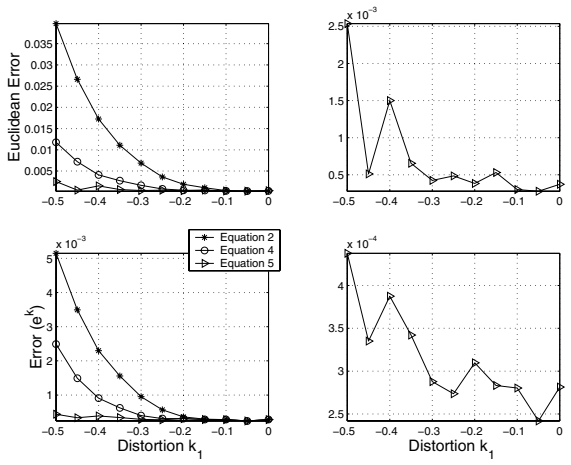

Figure 2. Normalised mean perimeter Euclidean errors for three methods.

Experiments on real images were carried out using two different wide angle lenses. Results are compiled on different images than those used during the estimation process, to show the quality of each models global approximation. Twenty independent samples of a planar target were taken and undistorted according with eq.(2), eq.(4) and eq.(5). Statistical moments of the mean perimeter errors of each sample are presented in table 1. Figure 3 shows an image undistorted using the proposed method. These results show improved distortion modelling and removal using the proposed model, and consistency between the behaviour on simulated and real data.

6mm Lens	Eq.2	Eq.4	**Eq.5**
Mean (norm)	6.5×10^{-4}	4.1×10^{-4}	3.3×10^{-4}
Mean (pixels)	0.83	0.52	0.42
Max (pixels)	1.60	0.85	0.64
Min (pixels)	0.38	0.33	0.148
FinePix $\approx$ 8mm	Eq.2	Eq.4	**Eq.5**
Mean (norm)	2.2×10^{-4}	1.9×10^{-4}	1.6×10^{-4}
Mean (pixels)	0.44	0.38	0.32
Max (pixels)	0.63	0.55	0.46
Min (pixels)	0.30	0.27	0.24

Table 1. Perimeter errors on real data.

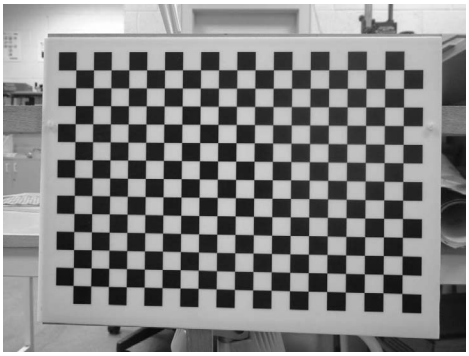

Figure 3. Undistorted image sample.

5. Conclusion

This paper deals with the precise removal of radial distortion from an image array. Initially, the distortion model is presented as a function of ideal or undistorted points. Consequently, an inverse function is required in order to undistort the image. A new inverse function is formed by a rearrangement of a first order taylor expansion. Implementation details for parameter estimation are also given. Theoretical and experimental results are compared to other inverse models proposed in the literature. They clearly indicate an improved performance, attaining sub-pixel accuracy over a wide range of distortion levels.

References

[1] K. Atkinson. *Close range photogrammetry and machine vision*. Whittles Publishing, 1996.

[2] M. Born and E. Wolf. *Principles of Optics*. Permagon, 6 edition, 1980.

[3] D. C. Brown. Decentering distortion of lenses. *Photogrammetric Engineering*, 32(3):444–462, 1966.

[4] D. C. Brown. Close-range camera calibration. *Photogrammetric engineering*, 37:855–866, 1971.

[5] A. Conrady. Decentering lens systems. *Monthly notices of the royal astronomical society of america*, 79:951–954, 1919.

[6] F. Devernay and O. D. Faugeras. Straight lines have to be straight. *Machine Vision and Applications*, 13(1):14–24, 2001.

[7] W. G. Driscoll and W. Vaughan. *Handbook of optics*. McGraw-Hill, 1978.

[8] J. G. Fryer and D. C. Brown. Lens distortion for close-range photogrametry. *Photogrammetric engineering and remote sensing*, 52(1):51–58, 1986.

[9] J. Heikkila. Geometric camera calibration using circular control points. *IEEE Transactions on Pattern Analysis and Machine Intelligence*, 22(10):1066–1077, 2000.

[10] J. Heikkila and O. Silven. A four-step camera calibration procedure with implicit image correction. In *CVPR97*, 1997.

[11] C. C. Slama. *Manual of photogrammetry*. American society of photogrammetry, 4 edition, 1980.

[12] G. P. Stein. Internal camera calibration using rotation and geometric shapes. Master's thesis, MIT, 1993.

[13] T. Tamaki, T. Yamamura, and N. Ohnishi. Unified approach to image distortion. In *ICPR02*, pages 584–587, 2002.

[14] T. Thormaehlen, H. Broszio, and I. Wassermann. Robust line-based calibration of lens distortion from a single view. In *Mirage 2003*, pages 105–112, 2003.

[15] R. Tsai. A versatile camera calibration technique for high accuracy 3d machine vision metrology using off-the-shelf tv cameras and lenses. *IEEE Journal of Robotics and Automation*, 3(4):323–344, 1987.

[16] K. Vijayan Asari, S. Kumar, and D. Radhakrishnan. A new approach for nonlinear distortion correction in endoscopic images based on least squares estimation. *IEEE Transactions on Medical Imaging*, 18(4):345–354, April 1999.

[17] G. Wei and S. Ma. Implicit and explicit camera calibration - theory and experiments. *IEEE Transactions on Pattern Analysis and Machine Intelligence*, 16(5):469–480, 1994.

[18] J. Weng, P. Cohen, and M. Herniou. Camera calibration with distortion models and accuracy evaluation. *IEEE Transactions on Pattern Analysis and Machine Intelligence*, 14(10):965–980, 1992.